RNA BIOLOGY
2025, VOL. 22, NO. 1, 1–9
https://doi.org/10.1080/15476286.2025.2449775

Taylor & Francis
Taylor & Francis Group

REVIEW

Expanding the immune-related targetome of miR-155-5p by integrating time-resolved RNA patterns into miRNA target prediction

Martin Hart[a,b], Caroline Diener[a], Stefanie Rheinheimer[a], Tim Kehl[c], Andreas Keller[d,e], Hans-Peter Lenhof[c], and Eckart Meese[a]

[a]Institute of Human Genetics, Saarland University (USAAR), Homburg, Germany; [b]Center of Human and Molecular Biology (ZHMB), Saarland University (USAAR), Saarbrücken, Germany; [c]Center for Bioinformatics, Saarland Informatics Campus, Saarland University (USAAR), Saarbrücken, Germany; [d]Chair for Clinical Bioinformatics, Saarland University (USAAR), Saarbrücken, Germany; [e]Helmholtz Institute for Pharmaceutical Research Saarland (HIPS)–Helmholtz Centre for Infection Research (HZI), Saarland University Campus, Saarbrücken, Germany

ABSTRACT

The lack of a sufficient number of validated miRNA targets severely hampers the understanding of their biological function. Even for the well-studied miR-155-5p, there are only 239 experimentally validated targets out of 42,554 predicted targets. For a more complete assessment of the immune-related miR-155 targetome, we used an inverse correlation of time-resolved mRNA profiles and miR-155-5p expression of early CD4+ T cell activation to predict immune-related target genes. Using a high-throughput miRNA interaction reporter (HiTmIR) assay we examined 90 target genes and confirmed 80 genes as direct targets of miR-155-5p. Our study increases the current number of verified miR-155-5p targets approximately threefold and exemplifies a method for verifying miRNA targetomes as a prerequisite for the analysis of miRNA-regulated cellular networks.

ARTICLE HISTORY
Revised 14 December 2024
Accepted 27 December 2024

KEYWORDS
miR-155-5p; CD4+ T cell activation; target prediction; time-resolved RNA patterns; miRnomics; transcriptomics

Introduction

Since the discovery of microRNAs (miRNAs, miRs) in 1993 by Lee, Feinbaum and Ambros [1], the post-transcriptional regulation of target mRNAs (messenger RNA) by miRNAs has been extensively studied. Towards a better understanding of these regulatory processes, the identification and validation of a targetome for a single miRNA remains a major challenge [2]. Potential microRNA target interactions (MTIs) can be predicted using a growing number of *in silico* tools [3]. Experimental validation of MTIs can be achieved by reporter assays or high-throughput methods such as CLIP-seq or CLASH [4]. The combination of immunoprecipitation of argonaute (AGO) family members with next-generation sequencing (AGO-HITS-CLIP) allows to identify an enormous number of MTIs [5]. However, the data derived from Ago-bound miR-mRNA-complexes do not necessarily allow the identification of functional MTIs [2,6].

There is a large number of different features contributing to the functionality of MTIs, including the secondary structures of 3'UTRs, thermodynamic binding stabilities and other context-specific factors such as miRNA:target ratios [2,7]. This complex situation contributes to relatively low target prediction accuracies (10–50%) of functional MTIs assays [8]. An example of this unsatisfactory situation is the targetome of miR-155-5p, which is one of the well-studied miRNAs in terms of inflammatory responses, cancer and other immune-related diseases [9–11]. Since its deposition in the miRbase in 2004, only 239 high confidence MTIs were deposited in the miRTarBase representing an average number of 11.95 MTIs per year [12–14].

Towards a more comprehensive characterization of the immune-related targetome of miR-155-5p, we analysed a total of 90 potential miR-155-5p targets for functional MITs. Potential targets were selected based on their inverse correlation with the expression of miR-155-5p during the activation of human CD4+ T cells [15] in combination with an *in-silico* target prediction [16].

Results

Combination of miR-155-5p target gene prediction and inverse correlation with time-resolved transcriptome data of early CD4+ T cell activation

In our former study on early human CD4+ T cell activation signalling, we identified a very strong increase of the miR-155-5p expression reaching from 40 to 1,600 molecules/cell during the first 24 h upon T cell activation [15]. Out of 535 potential target genes that were *in silico* predicted and additionally showed inverse correlating mRNA time-course patterns as compared to the miR-155-5p expression, we previously validated 17 as direct targets [15].

CONTACT Martin Hart martin.hart@uks.eu Institute of Human Genetics, Saarland University, Building 60, Homburg 66421, Germany
Supplemental data for this article can be accessed online at https://doi.org/10.1080/15476286.2025.2449775

For a comprehensive assessment of the immune-related miR-155-5p targetome, we extended our analysis to 90 additional target genes. According to our reported T cell expression data [15], the time-course fold changes of the corresponding mRNA targets ranged from 1.209 (*NECAB1;* N-terminal EF-hand calcium-binding protein 1) and 62.479 (*MS4A7;* membrane spanning 4-domains A7). For experimental target examination, a semi-automated, dual luciferase assay-based approach was applied that follows the recently introduced HiTmIR protocol [6]. Due to length restrictions of the utilized reporter plasmid (pMIR-RNL-TK), some 3'UTRs of the 90 target genes bearing multiple binding sites were split into several sections, so a total of 103 reporter constructs were included in the analysis (Supplementary Table S1) (Figure 1).

Analysis of the predicted inverse-correlated miR-155-5p target genes by HiTmIR

The 103 3'UTR sequences were synthesized and cloned into the pMIR-RNL-TK reporter vector. These reporter constructs were analysed by HiTmIR. A reporter plasmid, containing the *FOS* 3′ UTR (pMIR-FOS), served as a positive control. A co-transfection of miR-155-5p together with this positive control in HEK-293T cells resulted in a highly significant reduction of the relative light units (RLU) to 55.7% ($p < 0.001$) (Figure S1A).

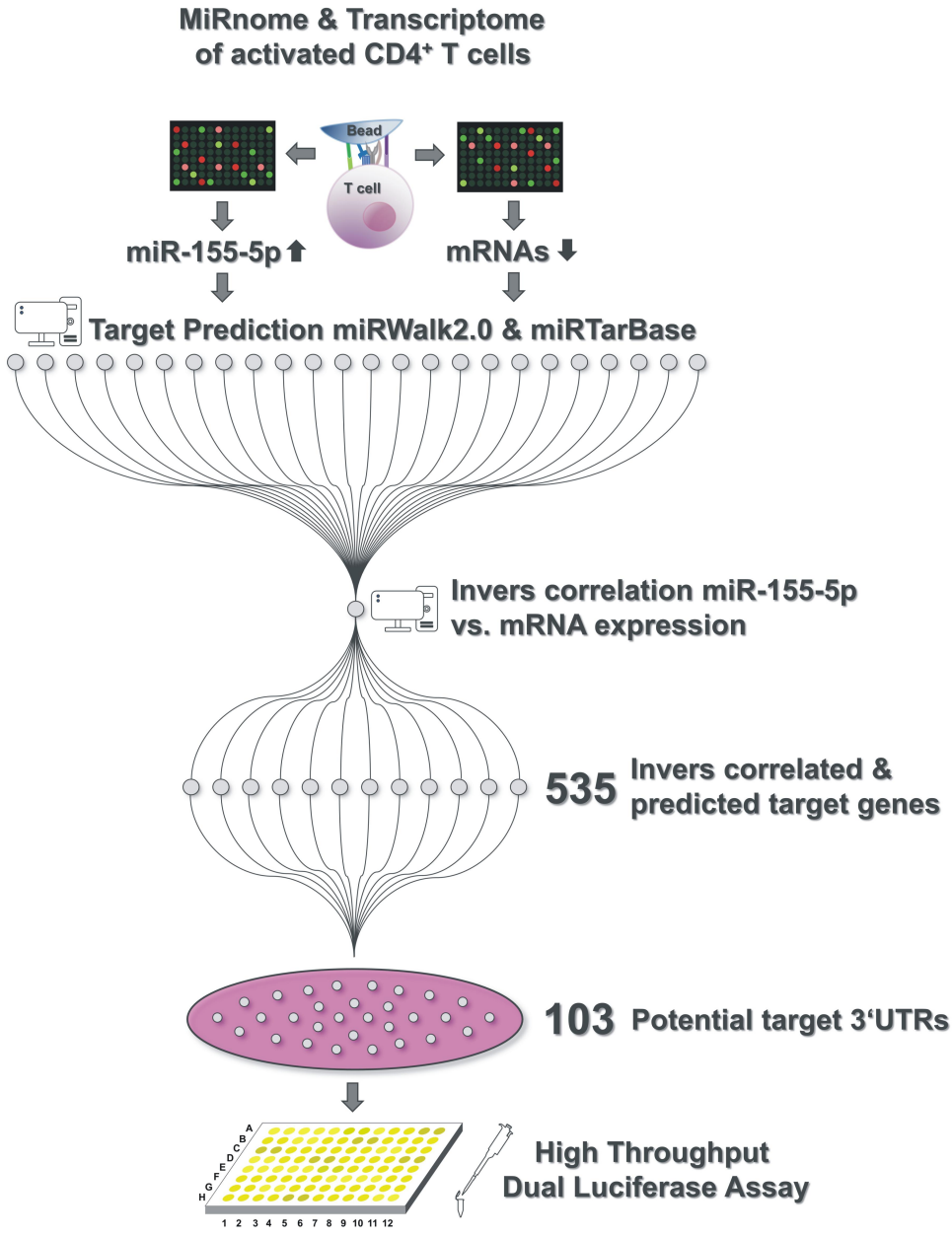

Figure 1. Implementation of time-resolved, inverse-correlated miRNA and mRNA expression data in prediction and validation by HiTmIR. Diener et al. investigated the time resolved mRNA and miRNA expression profiles of early CD4+ T cell activation [15]. We predicted the miR-155-5p target genes using miRwalk2.0 and used inverse correlation of the predicted target genes and the time resolved mRNA data for target prediction. For further validation by HiTmIR, we randomly chose 103 potential target gene 3'UTR sequences.

The 103 analysed reporter constructs have exhibited RLUs ranging from 34.9% to 124.8% upon miR-155-5p co-transfection (Figure 2a,b). The most pronounced significant RLU reduction to 34.9% was detected for *MPEG1* (macrophage expressed 1). For the stringent detection of positive MTIs we applied two criteria: i) RLU reduction of to less than 85% and ii) significant reduction of the RLU below a p-value of 0.05. This threshold was selected to determine positive target genes in a high confidential manner as described in our previous study [6]. Figure 2a displays all target gene 3'UTR constructs with RLUs less than 70% and Figure 2b all target gene 3'UTR constructs with RLUs more than 70%. Applying our criteria, we detected 87 target gene 3'UTR constructs with a significant reduction in the RLU of less than 85% (Figure 2d) resulting in a validation rate of 84.5% (Figure 2e). Only 2.9% of the reporter vectors displayed an RLU of less than 40% (Figure 2c). With 68.9% the majority of the reporter constructs showed a reduction in the RLU between 50% and 80%. For 10.7% of the reporter constructs, we detected an RLU ranging from 70% to 80%. and 7.8% revealed an RLU more than 90%. The mean RLUs of all initially tested reporter constructs are given in Supplementary Table S3. In comparison to the above-mentioned 239 target genes of miR-155-5p which are deposited in the miRTarBase, our analysis identified 80 direct target genes resulting in an overall increase of ~30% (Figure 2f). This prompted us to verify the results of the initial HiTmIR assays by mutagenesis of the respective miR-155-5p binding sites for selected reporter constructs.

Validation of miR-155-5p target genes by mutagenesis HiTmIR

For exemplary validation of the direct binding of miR-155-5p to its identified targets, we mutated the respective binding sites in the 3'UTRs of *MPEG1, ULK2, BORCS7, ARRDC2, DELE1* and *RCHY1* and tested these mutated reporter vectors with our Mutagenesis HiTmIR Assay. As aforementioned, the pMIR-FOS reporter vector served as a positive control. The co-transfection of miR-155-5p and the positive control in HEK-293T cells resulted in a highly significant reduction of the relative light units (RLU) to 59.6% ($p < 0.001$) (Figure 1b). As for the results of the initial testing series, all wild-type constructs showed a significant reduction of the RLU. The mutation of the binding sites of the reporter vectors reversed this effect, which verified the direct binding of miR-155-5p to its binding sites (Figure 3a).

Impact of the binding site type on the reduction of the RLU

To analyse the impact of the type of binding site on the RLU large datasets on a standardized platform are required. In this analysis, we implemented only canonical miR-155-5p binding sites (6-mer, 7mer-A1, 7mer-m8, 8-mer) from target 3'UTRs that harboured only a single binding site (Figure 3b). Consistent with published literature, we expected an RLU reduction in the following gradations from high to low reduction indices: 8-mer, 7mer-m8, 7mer-A1, 6-mer. For 6-mer binding sites, we detected the weakest effect with RLUs between 51.2% to 116.5% and 45.5% were negative target genes. RLUs of 7mer-A1 binding sites ranged between 38.8% to 101.4% and 13% of the target genes were negatively tested. 7mer-m8 binding sites displayed RLUs between 46.1% to 106.5% and 13% negative-tested reporter vectors. 8-mer binding sites exhibited the most pronounced decrease in the RLU with a mean reduction of 60% ranging from 42.8% to 101.3% with 8% negative target genes. Our results for miR-155-5p confirmed the prevailing scientific opinion.

Protein–protein interaction network analysis of miR-155-5p target genes mirrors pathways of early T cell activation

For the identification of miR-155-5p regulated pathways of the early CD4+ T cell activation we conducted a protein–protein association analysis using the STRING database with all inversely correlated mRNAs. With a validation rate of 84.5% of the tested target genes is legitimate to enclose all inversely correlated mRNAs in this analysis. We identified three distinct interaction networks with a false discovery rate ≥0.05 (Figure 4). In the Gene Ontology category 'Molecular Function', we identified the subcategory 'SMAD binding', in KEGG Pathways the subcategory 'FoxO signaling pathway' and in WikiPathways the 'IL-4 signaling pathway'.

Discussion

The posttranscriptional regulation of mRNA target genes by miRNAs is extensively studied with 40,759 publications in PubMed since 2001. In the last two decades ~1,772 studies per year were published dealing with this topic, corresponding to ~4.9 per day. Despite these exceeding efforts, the identification and validation of a targetome of a single miRNA is still pending. The efficient identification of MTIs starts with an *in-silico* target prediction to identify potential target genes of a miRNA. For example, our target prediction for miR-155-5p initially provided 42,553 potential target genes. The functional analysis of such an enormous number of targets is still not applicable. So, the development of more precise prediction tools is pivotal. The five key principles which are used for target prediction are sequence or seed complementary, structural and energetic properties, site accessibility, species conservation and expression analysis. For the latter principle, the expression analysis, tools like MMIA, CoMeTa and Cupid implemented miRNA and mRNA expression data searching for inverse correlations [17–19]. However, the updated version of MMIA from 2015, CoMeTa, which is not updated since its release in 2012 and Cupid, also not updated since its release in 2015, are limited in use by working partially with discontinued target prediction tools like miRecords [20].

Towards an improved prediction of MTIs, we combined an *in-silico* target prediction using miRWalk2.0 with time-resolved mRNA and miRNA expression data of activated CD4+ T cells. We hypothesized that implementing inverse correlation of longitudinal mRNA and miRNA expression data gained from time course experiments of activated cells in miRNA target prediction could reduce the number of false positive targets. We combined *in-silico* prediction of miR-155-

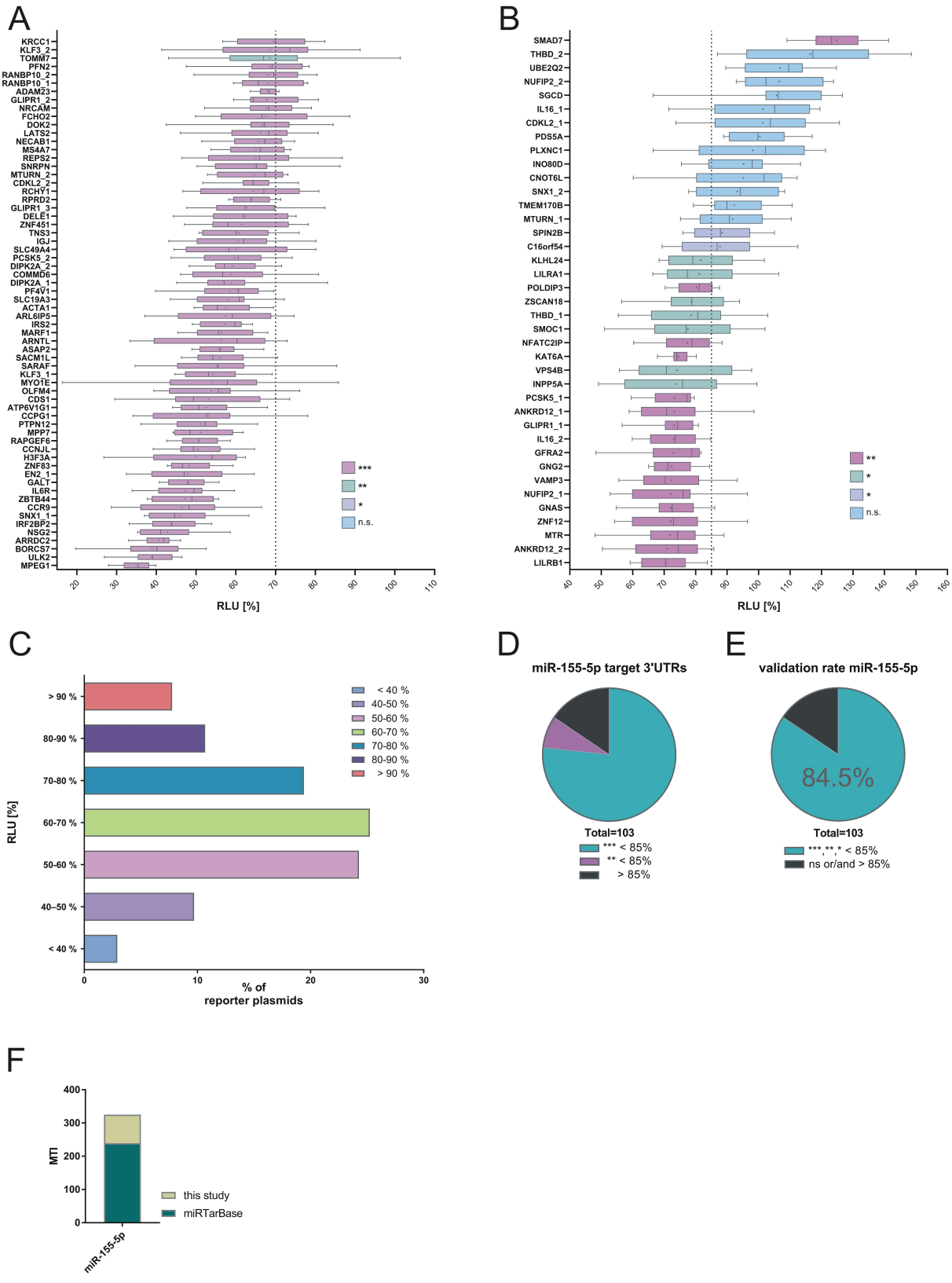

Figure 2. Analysis of the predicted inverse correlated miR-155-5p target genes by HiTmIR. (A): target genes with an RLU ≤ 70% and (B) target genes with an RLU ≥ 70%: HEK 293T cells were transfected with 50 ng/well of either reporter plasmid pMIR-RNL-TK, with or without insert, and 200 ng/well of miRNA expression plasmid containing either the respective miRNA or no insert. The RLU of the miR1555p transfected samples were normalized to the RLU measured with empty reporter vector. Four independent experiments were conducted in duplicates. Columns coloured in magenta show a significant reduction of the luciferase activity with a p-value ≤ 0.001. Columns coloured in green show a significant reduction of the luciferase activity with a p-value ≤ 0.01 and ≥0.001. Columns coloured in violet show a significant reduction of the luciferase activity with a p-value ≤0.05. Columns coloured in light blue show a non-significant reduction of the luciferase activity with a p-value ≥0.05. Data are shown as mean±sem. (C): distribution of the miR-155-5p effect on reporter plasmids. The analysed reporter plasmids were categorized by the detected RLU. (D): distribution of all positive target genes by RLU and p-value. Turquoise: highly significant reduction of RLU ≤ 85% with a p-value ≤ 0.001, magenta: significant reduction of RLU ≤ 85% with a p-value ≤ 0.01 and ≥0.001, Black: negative target genes. (E) Validation rate miR-155-5p. A positive target gene is defined by an RLU ≤ 85% with a p-value ≤ 0.01 (turquois). (F) Comparison of MTIs of miR-155-5p deposited in miRtarbase with positive MTIs from this study. Turquois: number of MTIs deposited in miRtarbase, Beige: number of positive MTIs from this study.

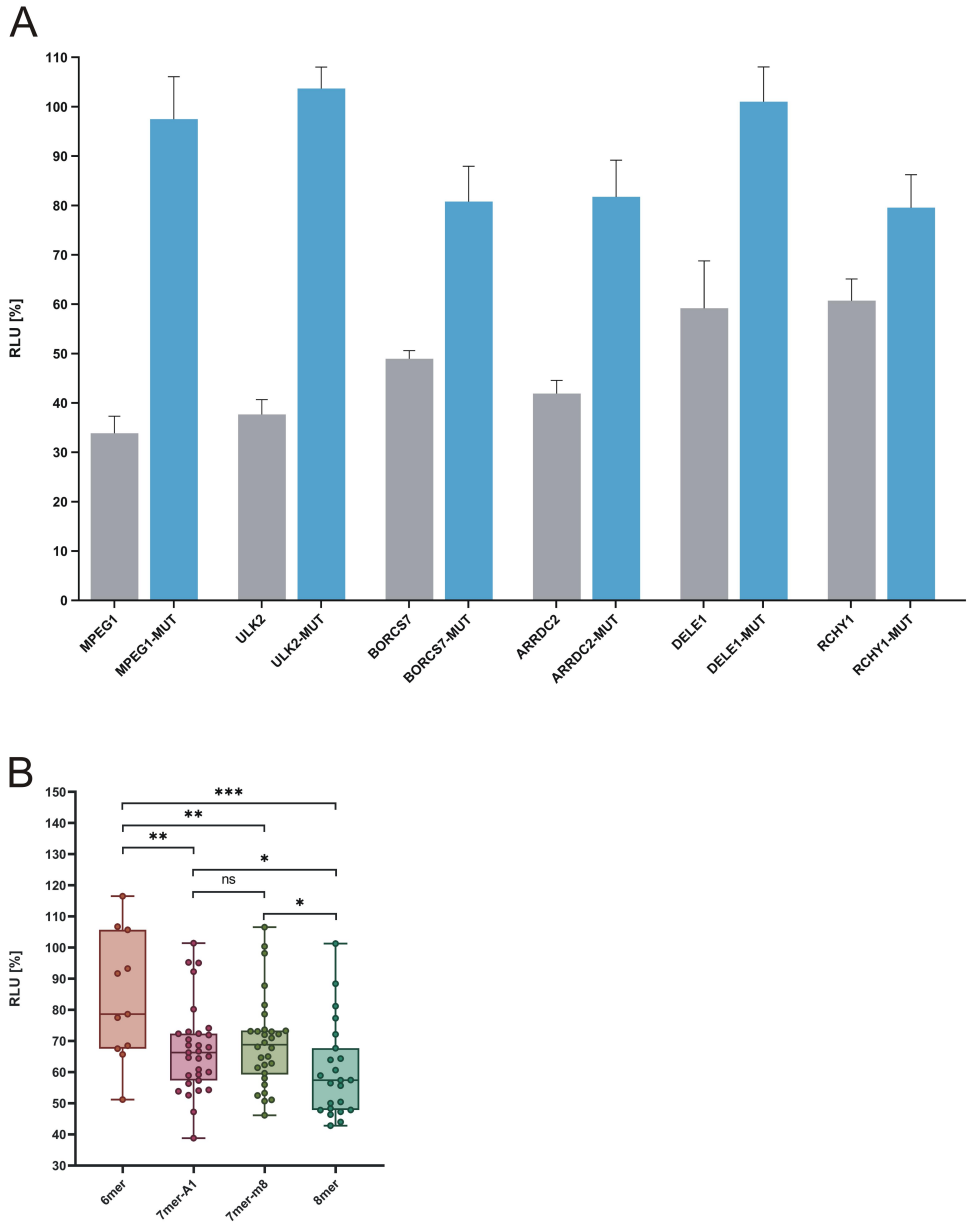

Figure 3. (A) validation of miR-155-5p target genes by mutagenesis HiTmIR. HEK 293T cells were co-transfected with miR-155-5p expression plasmids and wild-type reporter vectors of the respective target genes (light grey) or mutated reporter vectors (–mut) of the respective target genes (blue) as shown in the diagram. Three independent experiments were conducted in duplicates. Three asterisks represent a significant reduction of the RLU with a p-value ≤0.001. Two asterisks represent a significant reduction of the RLU with a p-value ≤0.01 and ≥ 0.001. One asterisk represents a significant reduction of the RLU with a p-value ≤0.05. (B) Association between binding site type and RLU reduction. The box coloured in brown represents 6-mer binding sites. The box coloured in magenta represents 7-mer-A1 binding sites. The box coloured in green represents 7-mer-m8 binding sites. The box coloured in turquoise represents 8-mer binding sites.

5p target genes with two filter criteria: i) inverse correlation of the respective mRNA in the time resolved mRNA dataset with Pearson's (PCC) and/or Spearman's correlation coefficient (SCC) of at least –0.8, ii) fold change of at least 1.2 compared to the non-activated CD4+ T cells. Implementing inverse correlation of time resolved RNA expression data in target prediction tremendously increases the validation rate up to 88.8%. In comparison to other prediction methods without inverse correlation of time resolved RNA data, the number of false positive predicted targets is reduced from ~50%–70% to 12.2%. Former studies report an estimated false positive rate of up to 70% for predictors like miRanda, TargetScan DianamicroT and PicTar (reviewed in [21]). Using time-resolved RNA patterns for prediction overcomes the shortcomings of a static approach, such as target prediction with inverse correlation of RNA data from a single time point. Furthermore, the use of time-resolved data analysing multiple time points offers the possibility to consider the dynamic changes of miRNA–target interactions for target prediction. However, like all predictions based on mRNA expression data, our method can only detect target genes that are regulated by mRNA decay, but excludes target genes whose mRNAs are not expressed in the analysed cell type and target genes, which are regulated on protein level. In our previous study on early human CD4+ T cell activation, miR-155-5p exhibited the most substantial induction. Thus, we emphasize

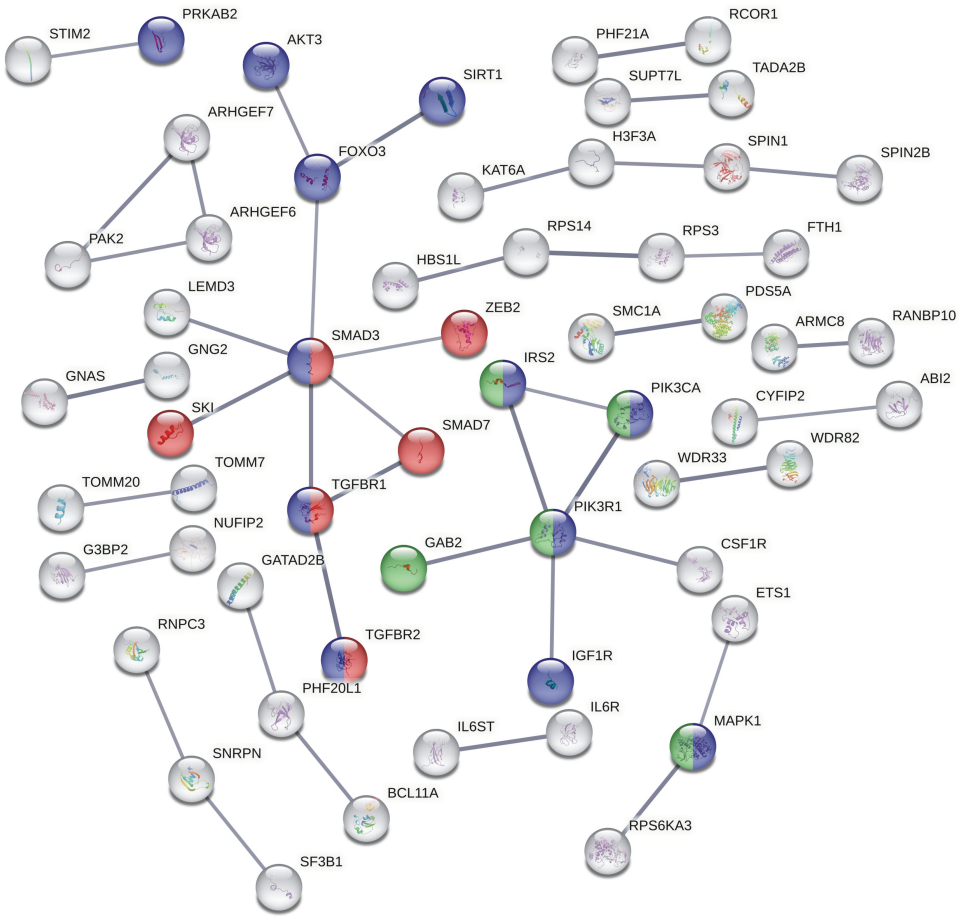

Molecular Function (Gene Ontology)			
GO Term	**Description**	**False Discovery Rate**	**Color**
0046332	SMAD binding	0.0248	Red
KEGG Pathways			
Pathway	**Description**	**False Discovery Rate**	**Color**
hsa04068	FoxO signaling pathway	0.0000981	Blue
WikiPathways			
Pathway	**Description**	**False Discovery Rate**	**Color**
Wp395	IL-4 signaling pathway	0.0216	Green

Figure 4. Protein–protein interaction networks of 535 inverse-correlated miR-155-5p targets using the STRING database version 11.5. The miR-155-5p targets genes which are associated with the displayed pathways are coloured as indicated in the diagram.

that the effectiveness of our approach in integrating time-resolved, inverse-correlated miRNA and mRNA expression data into miRNA target prediction likely depends on the expression levels of the analysed miRNAs upon induction of their transcription. For miRNAs with rather small expression changes after transcriptional induction, longitudinal inverse correlations between miRNA and mRNA expression may have a reduced impact on target prediction accuracy.

To evaluate the performance of our prediction method, we compared the miR-155-5p target genes that tested positive in this study and the predicted miR-155-5p target genes that showed an inverse correlation in the time-resolved mRNA dataset of Diener et al. [15] with the results of a study by Loeb et al. that identified miR-155-5p target genes using HITS-CLIP [22] on activated murine WT and mir-155 knockout CD4+ T cells. We found no significant overlap between the data sets of this study and the study by Diener et al. with the AGO2-bound miR-155-5p target genes of the study by Loeb et al. (Figure 2; Supplementary Table S4). This may be due to differences in the model organisms. Loeb et al. used murine CD4+ T cells, while Diener et al. studied early activation in

human CD4+ T cells. In addition, miRNA–target interactions are highly dynamic and HITS-CLIP data seem to represent only a snapshot of this complex process.

Regarding the accumulating evidence that miRNAs modulate complex networks of target genes in an orchestrated manner, our prediction method offers the possibility to accurately determine these networks downstream to the induction of specific pathways. Given the high accuracy of our prediction method in combination with our high-throughput assay for validation, a pathway analysis of the mRNAs inversely correlated with miR-155-5p identified IL4, FoxO and SMAD signalling as miR-155-5p modulated pathways upon early T cell activation. IL-4 represents a crucial cytokine for the determination of T cell fates [23]. Produced by naïve CD4+ T cells, IL-4 regulates the differentiation of T cells into IL-4–producing effector Th2 cells [23,24]. Thereby autocrine IL-4 promotes cell proliferation and survival accounting for preferential expansion of IL-4-producing Th2 cells [24]. The regulation of IL-4 signalling by miR-155-5p could attenuate this feedback loop. Foxo transcription factors are known regulators of T cell biology comprising T cell trafficking, naive T cell homoeostasis, effector and memory responses, as well as differentiation and function of Tregs [25]. FOXO1 and FOXO3 are known target genes of miR1555p [26,27]. The miR-155-5p mediated down-regulation of FOXO1 upon T cell activation could contribute to enhance differentiation and proliferation of the activated T cells. Following T cell activation SMAD4 is essential for T cell proliferation and promotes T cell function by integrating multiple pathways independent of TGF-β [28]. The SMAD pathway regulates the balanced differentiation of CD4+ T cells into inflammatory Th17 cells and suppressive FOXP3+ T regs [29]. MiR-155 gene expression is induced by binding of Smad4 to the promoter region [30]. These findings point out to a miR1555p mediated feedback mechanism in early T cell activation orchestrating precise T cell differentiation and proliferation.

By incorporating time-resolved, inverse-correlated miRNA and mRNA expression data into miRNA target prediction, we enhanced the efficacy of target prediction tools and significantly improved validation rates. Our approach enabled the identification of complex miR-155-5p target gene networks on the road to a miR-155-5p targetome of early CD4+ T cell activation. This deeper insight into how miRNAs modulate molecular signalling networks in immune cells provides a basis for the use of miRNAs or pathway inhibitors in precisely targeted molecular therapies of immune-related diseases like cancer and neurodegenerative disorders.

Materials and methods

Cell line

The human cell line HEK-293T (ACC 635) was purchased from the German collection of microorganisms and cell cultures (DSMZ). The HEK-293T cells were authenticated by STR typing by DSMZ. The cells were cultured in DMEM (Life Technologies, Darmstadt, Germany) with Penicillin (100 U/ml), Streptomycin (100 µg/ml) and 10% [v/v] FCS and sub-cultured twice a week for less than 3 months after receipt.

miRNA expression plasmid and reporter vectors

The pSG5-mir-155 expression plasmid was described by Graesser et al. [31]. The 103 3'UTR sequences of 90 miR-155-5p target genes were synthesized and cloned by GeneArt Gene Synthesis Services (Thermo Fisher, Waltham, USA) via *Spe*I, *Sac*I restriction sites into the pMIR-RNL-TK vector, which was described in Beitzinger et al. [32]. For target genes with long 3'UTRs (>1500 nt) and more than one predicted miR-155-5p binding site the 3'UTR sequences were split into two fragments. The identifiers of all cloned 3'UTRs (NM accession numbers) and their sequences are given in Supplementary Table S1. For validation of the positively tested target genes, respective binding sites were mutated. The mutated sequences were synthesized and cloned by GeneArt Gene Synthesis Services (Thermo Fisher, Waltham, USA) via *Spe*I, *Sac*I restriction sites into the pMIR-RNL-TK vector. The 3'UTR sequences of the mutated reporter constructs are given in Supplementary Table S2.

High-throughput miRNA interaction reporter assay (HiTmIR)

The HiTmIR assay was conducted as described previously [6]. In brief, 3.2×10^4 HEK-293T cells were seeded out in a 96-well plate using the liquid handling system epMotion® 5075 (Eppendorf, Hamburg, Germany). One day later, the cells were transfected with 50 ng/well of reporter plasmid pMIR-RNL-TK, either with or without 3'UTR insert, and 200 ng/well of miRNA expression plasmid containing either the respective miRNA or no insert. Forty-eight hours after transfection, the cells were lysed and measured on a GloMax Navigator microplate luminometer (Promega, Madison, WI, USA) with the Dual-Luciferase® Reporter Assay System (Promega, Madison, WI, USA). For the analysis of the relative light units (RLUs), the firefly luciferase activity of each wild type 3'UTR reporter plasmid was standardized by the activity of a constitutively expressed renilla luciferase (Ratio Firefly/Renilla). The standardized luciferase activity of each wild type 3'UTR reporter construct co-transfected with miR-155 was normalized/compared to the luciferase activity of the empty reporter vector co-transfected with miR-155. The luciferase assays were performed four times in technical duplicates. For the mutagenesis high-throughput miRNA interaction reporter assay (Mutagenesis HiTmIR) 24 h after seeding of the cells they were transfected with 50 ng/well of either reporter plasmid pMIR-RNL-TK, with or without or mutated insert and 200 ng/well of miRNA expression plasmid containing either the respective miRNA or no insert. The cells were lysed and measured as described above. The Mutagenesis HiTmIR Assays were performed in three independent experiments in technical duplicates. For statistical analysis of the reporter assays, we used GraphPad Prism 9 using the Welch's t-test. The pMIR-

FOS reporter vector serves as a positive control. *FOS* (Fos proto-oncogene, AP-1 transcription factor subunit) was validated as a direct target gene of miR-155-5p by Dunand-Sauthier et al. [33].

Web tools and data analysis

For statistical analysis, we used GraphPad Prism 9 (GraphPad Software, Inc.). The asterisks in the figures represent the statistical significance as calculated by Welch's t-test: *= $0.01 < p \leq 0.05$; ** = $0.001 < p \leq 0.01$; ***= $p \leq 0.001$. The protein–protein interaction network analysis was conducted with the STRING database version 11.5 (https://string-db.org/) [34] for all inverse-correlated mRNAs. The default settings were changed for the minimum required interaction score to 'high confidence (0.700)', active interaction sources were limited to 'experiments', and disconnected nodes in the network were hidden.

For the comparisons between the results of the studies by Loeb et al. [22], Diener et al. [15] with the results of this study (Hart et al.) we used Venny 2.1 (https://bioinfogp.cnb.csic.es/tools/venny/index.html). The study by Loeb et al. analysed the AGO2 bound miR-155 target mRNAs in wild-type mouse activated CD4+ T cells in relation to mir-155 knockout mouse activated CD4+ T cells. The study by Diener et al. investigated the time-resolved inverse correlation of miR-155 and its target mRNAs after activation of human CD4+ T cells. The results of these studies were compared to the positively tested miR-155-5p target mRNAs in this study.

Predictions of potential miRNA targets

The predictions of potential miR-155-5p targets and the evaluations of time-course RNA expression data, as described below, refer to our former study that integrated miRnome and transcriptome analyses during the early 24 h of the human CD4+ T cell activation process [15]. In brief, *in silico* prediction of endogenous 3′UTRs binding sites was performed using miRWalk 2.0 [16]. Choosing a minimum seed binding length of 6 nt, potential targets were filtered for a prediction by at least five of the overall 13 included target prediction algorithms (miRWalk, DIANAmT3.0, miRanda (2010), miRDB (2009), miRWalk, RNAhybrid (version 2.1), PICTAR4 (2006), PICTAR5 (2007), PITA (2008), RNA22 (2008), MicroT4, miRBridge and TargetScan5.1). As a decisive criterion for further consideration, inverse correlations (Pearson's (PCC) and/or Spearman′s correlation coefficients (SCC) ≤−0.8) were assumed between the time-course mRNA expression of the predicted targets and the expression levels of miR-155-5p [15].

Disclosure statement

No potential conflict of interest was reported by the authors.

Funding

The work was supported by the Medical Faculty of Saarland University [HOMFOR2021] to Martin Hart.

Authors' contributions

M.H.: design of the work, acquisition, analysis, interpretation of data, drafted the work, C.D.: acquisition, analysis; S.R.: acquisition, analysis; T. K.: interpretation of data; A.K.: interpretation of data; HP.L.: interpretation of data; E.M.: design of the work, interpretation of data, drafted the work

Data availability statement

All data generated or analysed during this study are included in this published article and its supplementary information files.

References

[1] Lee RC, Feinbaum RL, Ambros V. The C. elegans heterochronic gene lin-4 encodes small RNAs with antisense complementarity to lin-14. Cell. 1993;75(5):843–854. doi: 10.1016/0092-8674(93)90529-Y

[2] Diener C, Keller A, Meese E. The miRNA–target interactions: an underestimated intricacy. Nucleic Acids Res. 2023;52(4):1544–1557. doi: 10.1093/nar/gkad1142

[3] Kern F, Backes C, Hirsch P, et al. What's the target: understanding two decades of in silico microRNA-target prediction. Brief Bioinform. 2020;21(6):1999–2010. doi: 10.1093/bib/bbz111

[4] Thomson DW, Bracken CP, Goodall GJ. Experimental strategies for microRNA target identification. Nucleic Acids Res. 2011;39(16):6845–6853. doi: 10.1093/nar/gkr330

[5] Kuhn DE, Martin MM, Feldman DS, et al. Experimental validation of miRNA targets. Methods. 2008;44(1):47–54. doi: 10.1016/j.ymeth.2007.09.005

[6] Kern F, Krammes L, Danz K, et al. Validation of human microRNA target pathways enables evaluation of target prediction tools. Nucleic Acids Res. 2021;49(1):127–144. doi: 10.1093/nar/gkaa1161

[7] Schaefer M, Nabih A, Spies D, et al. Global and precise identification of functional miRNA targets in mESCs by integrative analysis. EMBO Rep. 2022;23(9):e54762. doi: 10.15252/embr.202254762

[8] Sethupathy P, Megraw M, Hatzigeorgiou AG. A guide through present computational approaches for the identification of mammalian microRNA targets. Nat Methods. 2006;3(11):881–886. doi: 10.1038/nmeth954

[9] Hu J, Huang S, Liu X, et al. miR-155: an important role in inflammation response. J Immunol Res. 2022;2022:1–13. doi: 10.1155/2022/7437281

[10] Mahesh G, Biswas R. MicroRNA-155: a master regulator of inflammation. J Interferon Cytokine Res. 2019;39(6):321–330. doi: 10.1089/jir.2018.0155

[11] Mashima R. Physiological roles of miR-155. Immunology. 2015;145(3):323–333. doi: 10.1111/imm.12468

[12] Kozomara A, Birgaoanu M, Griffiths-Jones S. miRbase: from microRNA sequences to function. Nucleic Acids Res. 2019;47(D1):D155–D62. doi: 10.1093/nar/gky1141

[13] Kasashima K, Nakamura Y, Kozu T. Altered expression profiles of microRNAs during tpa-induced differentiation of HL-60 cells. Biochem Biophys Res Commun. 2004;322(2):403–410. doi: 10.1016/j.bbrc.2004.07.130

[14] Chou CH, Shrestha S, Yang CD, et al. miRtarbase update 2018: a resource for experimentally validated microRNA-target interactions. Nucleic Acids Res. 2018;46(D1):D296–D302. doi: 10.1093/nar/gkx1067

[15] Diener C, Hart M, Kehl T, et al. Quantitative and time-resolved miRNA pattern of early human T cell activation. Nucleic Acids Res. 2020;48(18):10164–10183. doi: 10.1093/nar/gkaa788
[16] Dweep H, Gretz N. miRwalk2.0: a comprehensive atlas of microRNA-target interactions. Nat Methods. 2015;12(8):697. doi: 10.1038/nmeth.3485
[17] Nam S, Li M, Choi K, et al. MicroRNA and mRNA integrated analysis (MMIA): a web tool for examining biological functions of microRNA expression. Nucleic Acids Res. 2009;37(suppl_2): W356–62. doi: 10.1093/nar/gkp294
[18] Gennarino VA, D'Angelo G, Dharmalingam G, et al. Identification of microRNA-regulated gene networks by expression analysis of target genes. Genome Res. 2012;22(6):1163–1172. doi: 10.1101/gr.130435.111
[19] Chiu HS, Llobet-Navas D, Yang X, et al. Cupid: simultaneous reconstruction of microRNA-target and ceRNA networks. Genome Res. 2015;25(2):257–267. doi: 10.1101/gr.178194.114
[20] Xiao F, Zuo Z, Cai G, et al. miRecords: an integrated resource for microRNA-target interactions. Nucleic Acids Res. 2009;37 (Database):D105–10. doi: 10.1093/nar/gkn851
[21] Muniategui A, Pey J, Planes FJ, et al. Joint analysis of miRNA and mRNA expression data. Brief Bioinform. 2013;14(3):263–278. doi: 10.1093/bib/bbs028
[22] Loeb GB, Khan AA, Canner D, et al. Transcriptome-wide miR-155 binding map reveals widespread noncanonical microRNA targeting. Mol Cell. 2012;48(5):760–770. doi: 10.1016/j.molcel.2012.10.002
[23] Silva-Filho JL, Caruso-Neves C, Pinheiro AAS. IL-4: an important cytokine in determining the fate of T cells. Biophys Rev. 2014;6 (1):111–118. doi: 10.1007/s12551-013-0133-z
[24] Keegan AD, Leonard WJ, Zhu J. Recent advances in understanding the role of IL-4 signaling. Fac Rev. 2021;10:71. doi: 10.12703/r/10-71
[25] Luo CT, Li MO. Foxo transcription factors in T cell biology and tumor immunity. Semin Cancer Biol. 2018;50:13–20. doi: 10.1016/j.semcancer.2018.04.006
[26] Ren L, Zhao Y, Huo X, et al. MiR-155-5p promotes fibroblast cell proliferation and inhibits FOXO signaling pathway in vulvar lichen sclerosis by targeting FOXO3 and CDKN1B. Gene. 2018;653:43–50. doi: 10.1016/j.gene.2018.01.049
[27] Hou L, Chen J, Zheng Y, et al. Critical role of miR-155/FoxO1/ROS axis in the regulation of non-small cell lung carcinomas. Tumour Biol. 2016;37(4):5185–5192. doi: 10.1007/s13277-015-4335-9
[28] Gu AD, Zhang S, Wang Y, et al. A critical role for transcription factor Smad4 in T cell function that is Independent of transforming growth factor β receptor signaling. Immunity. 2015;42 (1):68–79. doi: 10.1016/j.immuni.2014.12.019
[29] Malhotra N, Kang J. SMAD regulatory networks construct a balanced immune system. Immunology. 2013;139(1):1–10. doi: 10.1111/imm.12076
[30] Elton TS, Selemon H, Elton SM, et al. Regulation of the MIR155 host gene in physiological and pathological processes. Gene. 2013;532(1):1–12. doi: 10.1016/j.gene.2012.12.009
[31] Barth S, Pfuhl T, Mamiani A, et al. Epstein-Barr virus-encoded microRNA miR-BART2 down-regulates the viral DNA polymerase BALF5. Nucleic Acids Res. 2008;36(2):666–675. doi: 10.1093/nar/gkm1080
[32] Beitzinger M, Peters L, Zhu JY, et al. Identification of human microRNA targets from isolated argonaute protein complexes. RNA Biol. 2007;4(2):76–84. doi: 10.4161/rna.4.2.4640
[33] Dunand-Sauthier I, Santiago-Raber ML, Capponi L, et al. Silencing of c-Fos expression by microRNA-155 is critical for dendritic cell maturation and function. Blood. 2011;117 (17):4490–4500. doi: 10.1182/blood-2010-09-308064
[34] Szklarczyk D, Gable AL, Lyon D, et al. STRING v11: protein–protein association networks with increased coverage, supporting functional discovery in genome-wide experimental datasets. Nucleic Acids Res. 2019;47(D1):D607–D13. doi: 10.1093/nar/gky1131